Investigation of flow in axial stage of experimental turbine

Petr Straka[1,*], *Jaroslav* Pelant[1], *Martin* Němec[1], *Tomáš* Jelínek[1], and *Petr* Milčák[2]

[1]Aerospace Research and Test Establishment, Plc., Beranových 130, 19905 Prague – Letňany, Czech Republic
[2]Dossan Škoda Power Co., Ltd., Tylova 1/57, 30128 Plzeň, Czech Republic

Abstract. The contribution deals with investigation of flow in the axial stage of the experimental turbine with reaction blading. The main intention is to evaluate an effect of the secondary flows on the efficiency. Most important source of the secondary flows is an outflow from the seal above the rotor shroud. Other sources of the secondary flows are axial gaps between the rotor disc and the side walls of the stator blade channel and the outlet diffuser. Results of the numerical simulation are compared with the experimental data. In this work there is also studied possibility of transfer the outlet dissipation structures at the inlet of the stage as an approach to modelling of the multistage configuration.

1 Introduction

Flow in an axial turbine stage of an experimental turbine is investigated under the project of applied research TA04020129 [1], which deals with research of flow in multistage configuration of the axial turbine stages.

In case of multistage configuration of the axial turbine stage the inlet flow field to the stage is influenced by the flow through previous stages. Affected are primarily peripheral parts of the span.

In initial stage of the project TA04020129 [1] it was studied a simple possibility of modification of the measuring stand [2] for axial turbine stages in single stage configuration. The influence of previous stages was simulated by increasing of the boundary layer thickness on the side walls of the inlet diffuser and by adding the turbulizing grid inside the inlet diffuser. Some results of the numerical simulation and the experimental investigation can be found in [3,4].

The influence of previous stages is in this work simulated using transfer of the radial distribution of the outlet flow field parameters to the inlet boundary of the same stage. This approach is, of course, feasible only using numerical simulation, but not experimentally. Figure 1 shows a scheme of transfer of the outlet flow field parameters to the inlet boundary of the computational domain. In this work it is used the approach where the radial distributions of the normalized dynamic pressure $p_{\mathrm{dyn.,norm.}}$, the turbulence intensity Tu, the velocity vector angle in the tangential plane α and the velocity vector angle in the meridian plane γ are transferred from chosen section in the outlet part of the axial turbine stage to the inlet boundary. The normalized dynamic pressure is the ratio of the difference between

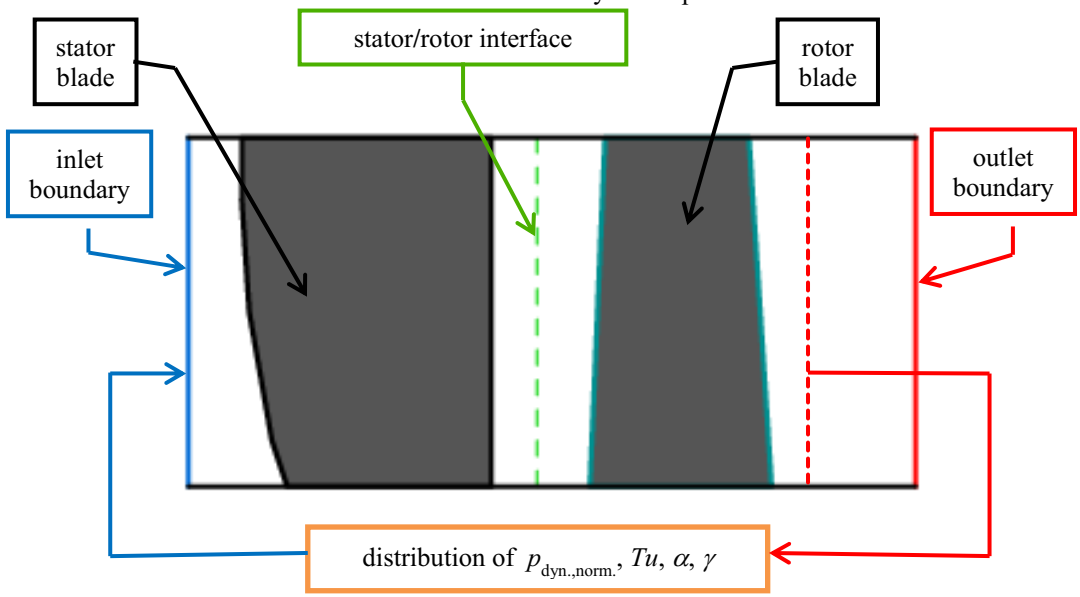

Fig. 1. Scheme of transfer of the outlet flow field parameters to the inlet boundary.

* Corresponding author: straka@vzlu.cz

the total pressure and the static pressure to the maximum value at given section. The fact, that the inlet and the outlet sections may have different dimensions, is respected using a scaling method. The calculation of flow in the axial turbine stage is performed iteratively. In the first step it is performed calculation without influence of previous stages, as the stage would be the first in a row. Then the radial distributions of $p_{\mathrm{dyn.,norm.}}$, Tu, α, γ are evaluated in chosen outlet section. In the next step there is performed calculation of flow with prescribed radial distributions of $p_{\mathrm{dyn.,norm.}}$, Tu, α, γ at the inlet boundary of the computational domain, as the stage would be the second in a row. The cycle can be repeated several times to simulate the order of the axial turbine stage in multistage configuration. Results of calculations of flow through the axial turbine stage called "REAC_v2-2", which is one of several configurations of reaction turbine stages designed in Doosan Škoda Power company and which are investigated under the project TA04020129 [1], are presented in this work.

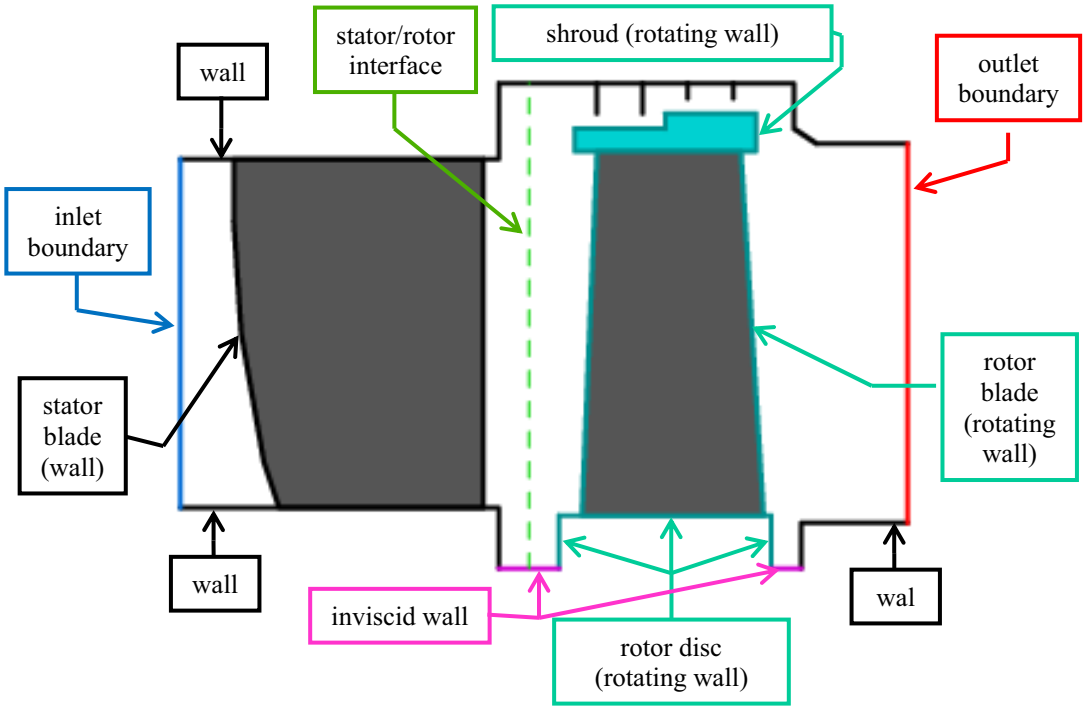

Fig. 2. Scheme of the computational domain.

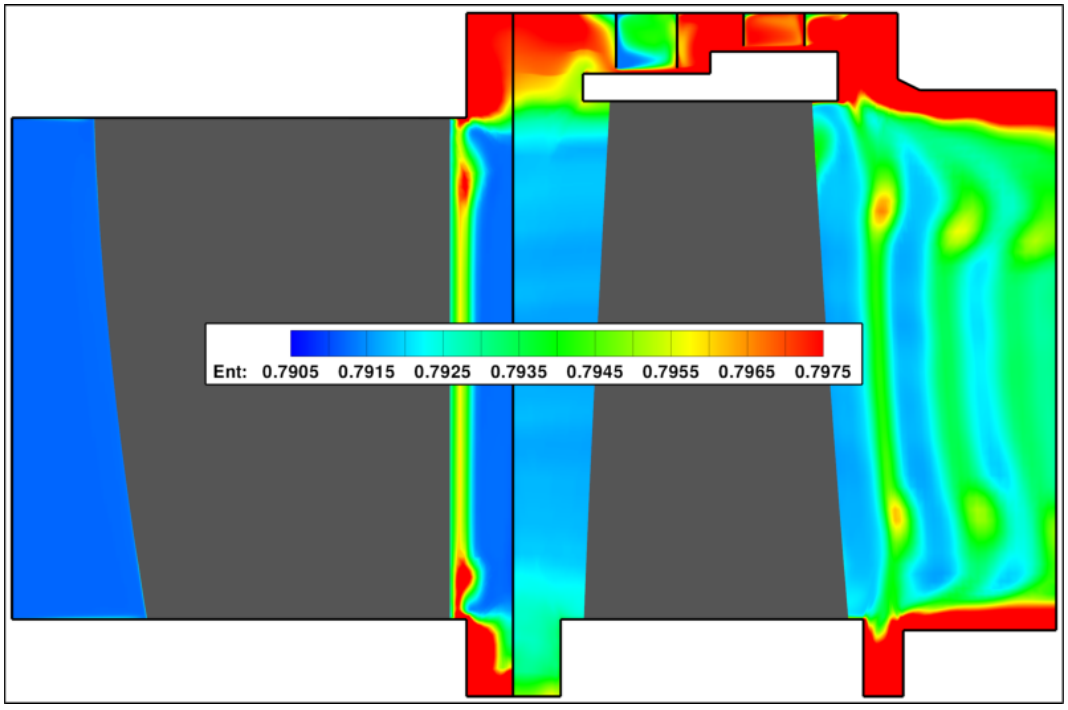

Fig. 3. Distribution of the normalized entropy index (Ent = p / ρ^{κ}) in meridian section in case without simulation of influence of the previous stage.

Calculations of flow were performed using the in-house numerical software, which is based on solution of RANS equations closed with two-equations turbulence model (for more details see [5,6,7]). The nonlinear explicit algebraic model of the Reynolds stress is used in this work [8]. The flowing medium is diatomic perfect gas. In figure 2 there is shown a scheme of the computational domain with highlighting the types of the boundary condition on various parts of the boundary. We can see that the rotor blade is equipped with the shroud. In the area above the shroud we can see the strips of the above-shroud seal. The rotor blades are carried on the rotating disc. Between the hub-wall of the stator and the rotor disc as well as between the rotor disc and the hub-wall of the outlet diffuser there are an axial gaps. These axial gaps are in this work replaced by cavities with a depth of about 15% blade height. On the bottom side of these cavities there is prescribed the slip boundary conditions (so called "inviscid wall"). The inlet boundary of the computational domain is placed in distance about 20% of the axial chord of the stator blade in front the stator leading edge (on the tip-diameter). The outlet boundary of the computational domain is placed in distance about 80% of the axial chord of the rotor blade behind the rotor trailing edge (on the hub-diameter). The axial distance between the stator trailing edge and the rotor leading edge (on the hub-diameter) is about 25% of the blade height. This dimension corresponds to the experimental configuration, where the flow field behind the stator wheel was traversed by the pneumatic probes. The radial gap between the rotor shroud and the strips of the above-shroud seal is about 1.06% of the blade height. The plane of evaluation of the radial distribution of the outlet flow field parameters was chosen in distance above 30% of the axial chord of the rotor blade behind the rotor trailing edge (on the hub-diameter). The radial

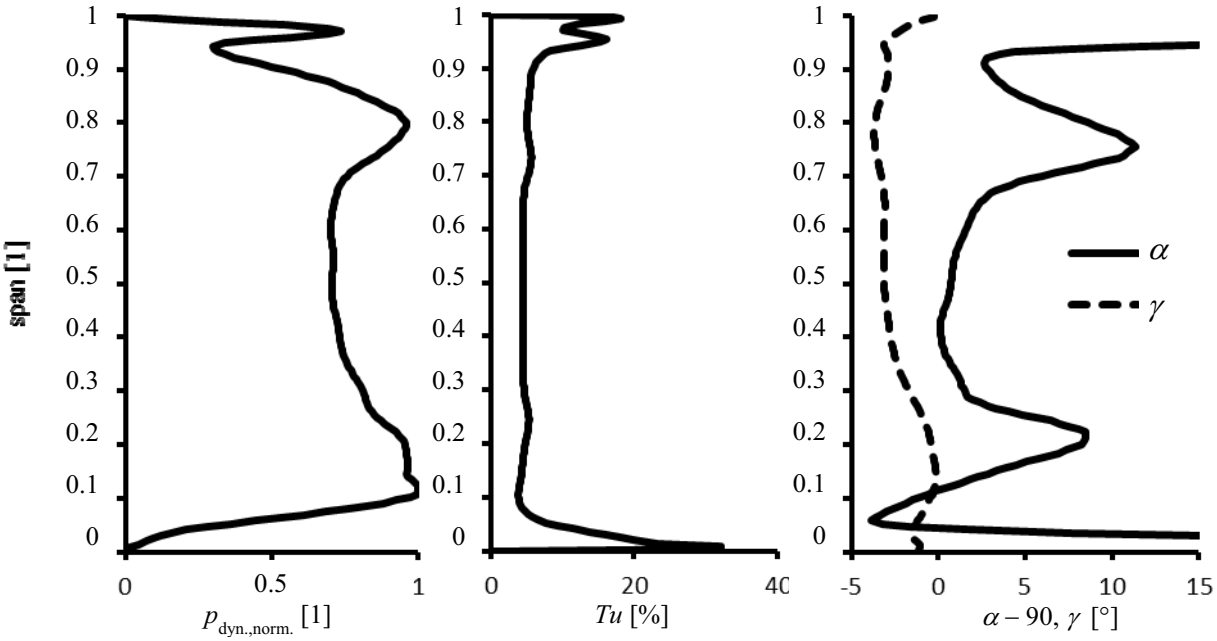

Fig. 4. Radial distribution of $p_{dyn.,norm.}$, Tu, α, γ.

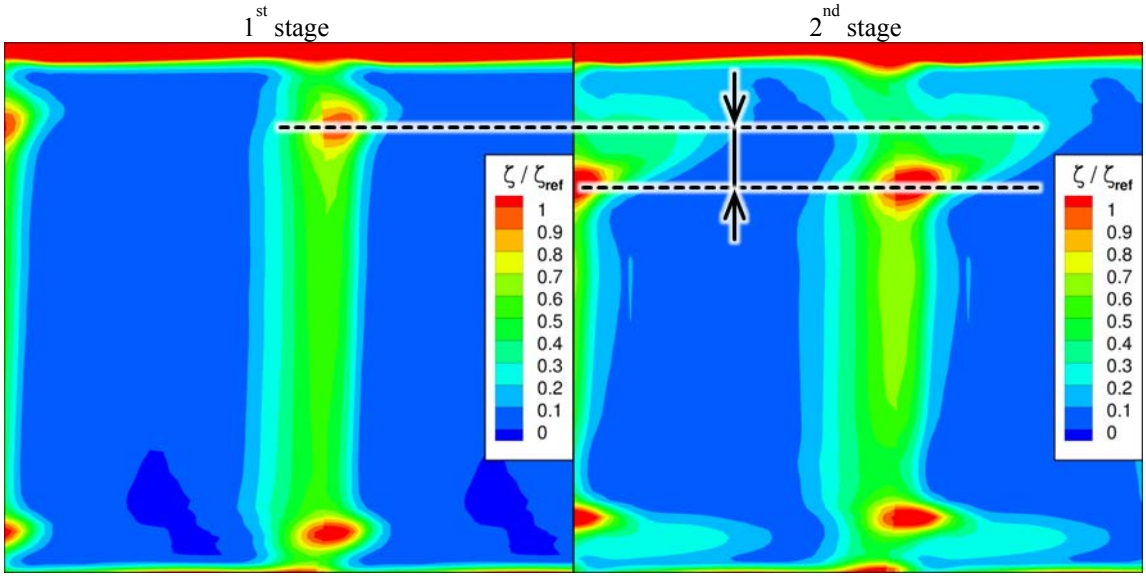

Fig. 5. Field of normalized kinetic energy losses in section behind the stator blades.

distribution of the outlet flow field parameters in this plane is influenced by the flow across the axial gap between the rotor disc and the hub-wall of the outlet diffuser and in tip-region it is influenced by the stream from the above-shroud seal.

2 Results

Flow in the axial turbine stage "REAC_v2-2" was calculated for the pressure ratio $p_{T0} / p_{S2} = 1.065$ (p_{T0} is the inlet total pressure, p_{S2} is the static outlet pressure), the velocity ratio $u / c_{2is} = 0.61$ (u is the circumferential speed, c_{2is} is the outlet isentropic velocity), the outlet isentropic Mach number $M_{2is} = 0.299$, revolution speed 2159.7 RPM, the total inlet pressure $p_{T0} = 100.931$ kPa, the total inlet temperature $T_{T0} = 297.5$ K. For calculation without the simulation of influence of previous stages the inlet turbulence intensity $Tu_0 = 5\%$ and the axial direction of the velocity vector were chosen.

In figure 3 there is shown field of the non-dimensional entropy index (p / ρ^{κ}, where p is the pressure, ρ is the density and κ is the adiabatic exponent) in the meridian section in case of flow without the simulation of influence of previous stages. Note here that all flow fields in this work are shown in normalized cylindrical coordinates (x / x_{ref}, φ / φ_{ref}, r / r_{ref}) instead of the Cartesian coordinates (x, y, z). The entropy index shows the dissipative structures in the flow field. It is clear that the major dissipation occurs due to flow through the above-shroud seal, due to mixing the stream from the above-shroud seal with the main stream in blade channel and due to flow across the axial gap before and behind the rotor disc. In Figure 3 there is also possible to detect projections of wakes to the meridian plane.

In figure 4 there are shown radial distributions of the normalized dynamic pressure $p_{dyn.,norm.}$, the turbulence intensity Tu and the velocity vector angles α and γ in section placed in distance above 30% of the axial chord of the rotor blade behind the rotor trailing edge (on the

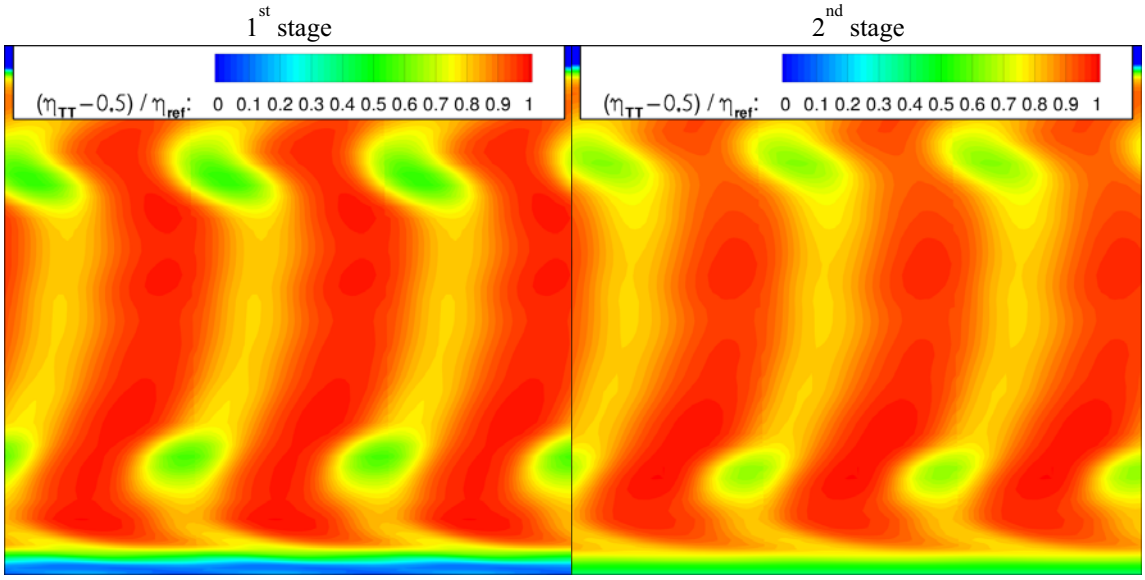

Fig. 6. Field of normalized total-total efficiency in section behind the stator blades.

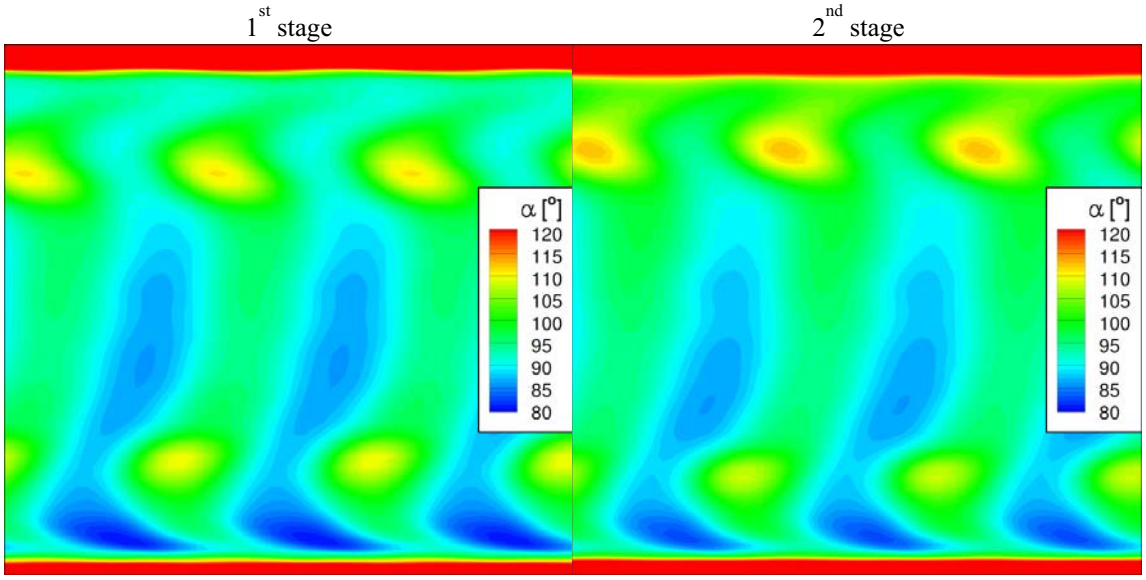

Fig. 7. Field of velocity vector angle α in section behind the stator blades.

hub-diameter). These distributions are evaluated from calculation without the simulation of influence of previous stages and are used for the inlet boundary condition in calculation of flow in stage which would be the second in a row in multistage configuration.

Way, how to prescribe the radial distribution of the turbulence intensity Tu and velocity angles α, γ, is straightforward. The radial distribution of the normalized dynamic pressure is used to define the local value of the total pressure on the inlet boundary: $p_T(r,\varphi) = p_S(r,\varphi) + p_{\text{dyn.,norm.}}(r)\ [p_{T0} - p_S(r,\varphi)]$. Note that (r, φ) are the cylindrical coordinates, p_{T0} is prescribed value of the inlet total pressure and p_S is local value of the static pressure which is extrapolated from the computational domain to the inlet boundary.

The influence of previous stage on the flow field in the second stage in multistage configuration is shown in figure 5 where is shown field of normalised kinetic energy losses in the axial gap between the stator and the rotor in plane placed in distance of 2 mm behind the stator trailing edge. From figure 5 it is clear that the previous stage causes increasing of the kinetic energy losses in peripheral parts of the span and it also causes shift of location of maximum value of the kinetic energy losses in wake in tip area. This demonstrates that there is an effect on development of the secondary vortices inside the inter-blade channel in tip area of the stator blades. The influence of the previous stage on the flow field at the outlet from the second stage is documented in figures 6 to 9. Figures 6, 7 and 8 show fields of the normalized total-total efficiency and two angles of the velocity vector (in tangential and meridian plane) in plane located in distance of 8 mm behind the rotor blade trailing edge (on the hub-diameter). The total-total

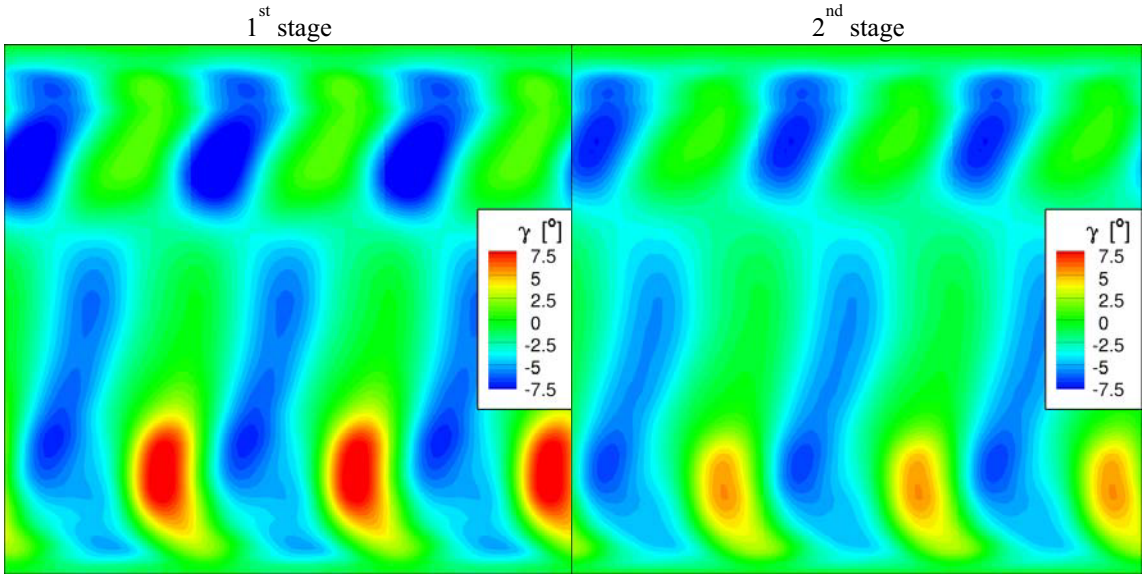

Fig. 8. Field of velocity vector angle γ in section behind the stator blades.

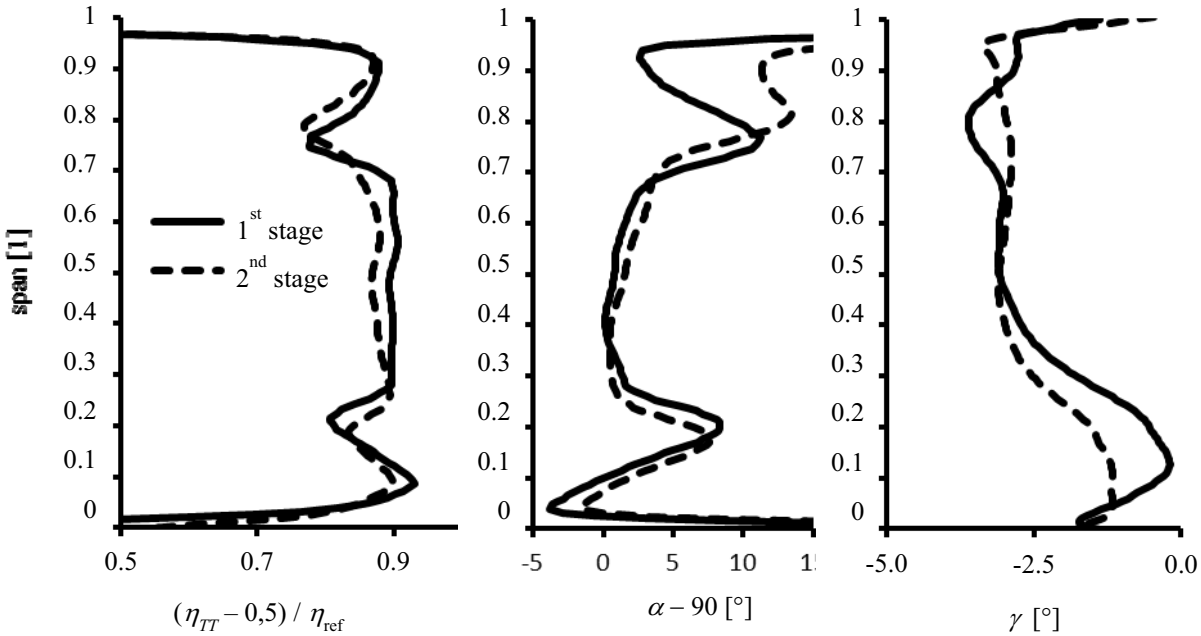

Fig. 9. Radial distribution of normalized total-total efficiency and two angles of the velocity vector (in tangential and the meridian plane) in a section behind the rotor blades.

efficiency is defined as $\eta_{TT} = (T_{T0} - T_T) / (T_{T0} - T_{Tis})$ where T_{T0} is the inlet total temperature, T_T is local total temperature and T_{Tis} is the total isentropic temperature.

On fields of the normalized total-total efficiency there are not apparent any significant differences between the first and the second stage in a row. I case of the angle α there are some differences in upper part of the span, whilst in case of the angle γ there are some differences in lower part of the span. This shows also figure 9 where are shown radial distributions of the circumferentially averaged values.

Figures 10 and 11 illustrate the influence of previous stages on flow field in axial turbine stage, which would be the third in multistage configuration. In figure 10 there is shown field of normalised kinetic energy losses in the axial gap between the stator and the rotor in plane placed in distance of 2 mm behind the stator trailing edge. From figure 10 it is evident that once again there is a change in the position of maximum of the kinetic energy losses in wake in the tip area. However, the difference between the second and third stage is not nearly as great as the difference between the first and second stage. This is also documented in figure 11 where are shown radial distributions of circumferentially averaged normalized total-total efficiency and two angles of the velocity vector in plane located 8 mm behind the trailing edge of the rotor blade (on the hub-diameter). Figure 11 demonstrates that the outlet flow field from the second stage in a row is almost identical with the outlet flow field from the third stage in a row in multistage configuration. Therefore, it can be assumed that the simulation of the fourth stage in a row should not already yield any new information.

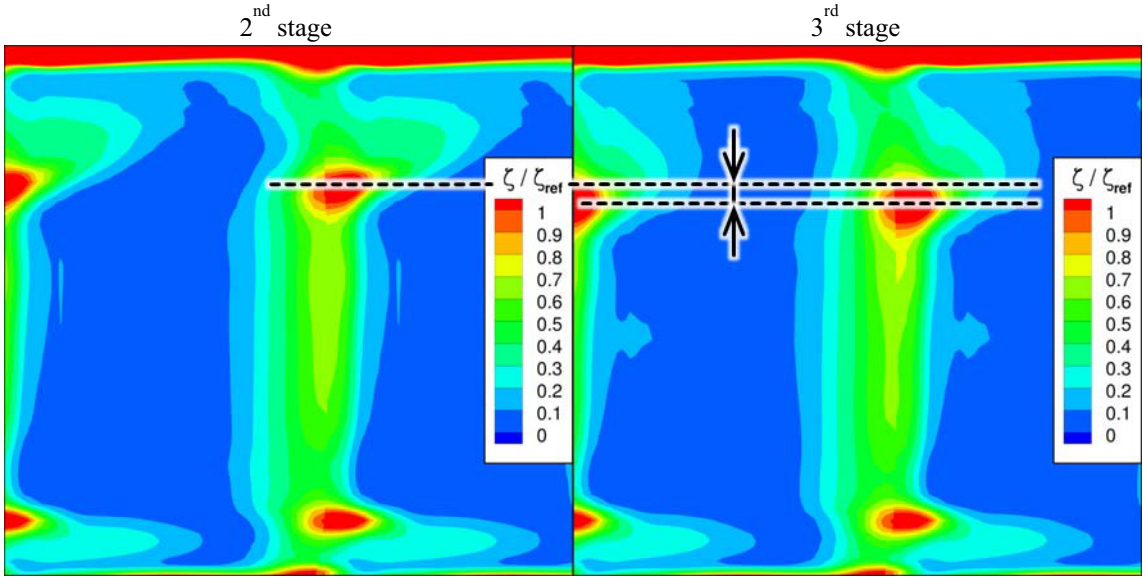

Fig. 10. Field of normalized kinetic energy losses in section behind the stator blades.

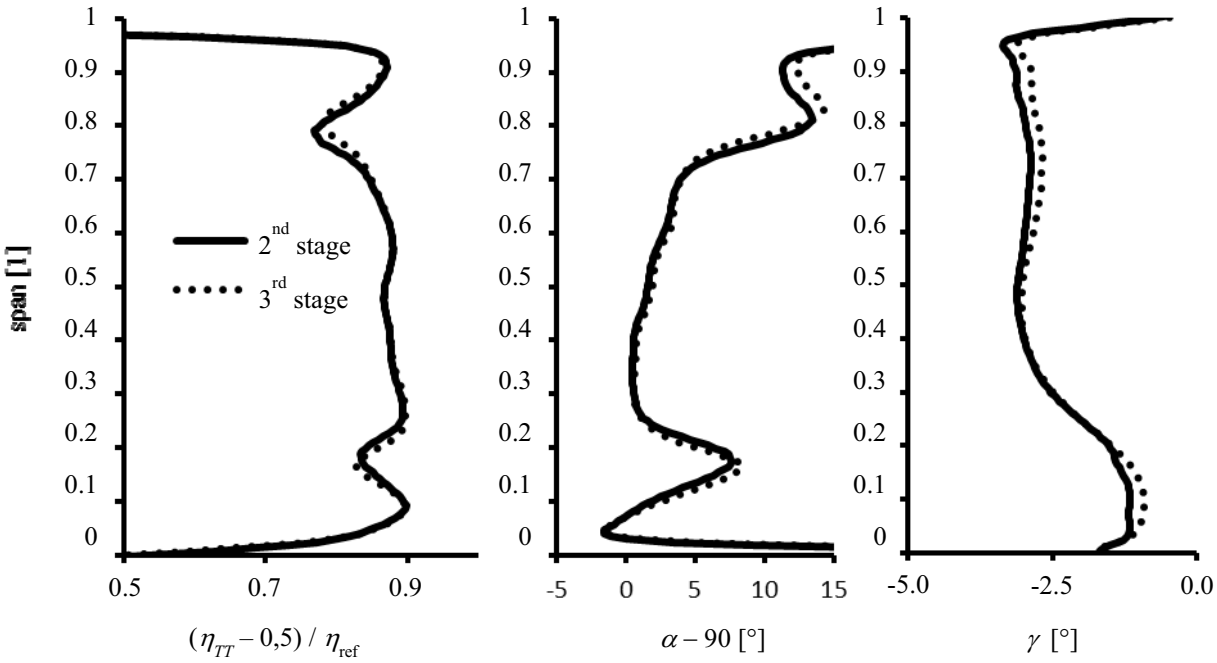

Fig. 11. Radial distribution of normalized total-total efficiency and two angles of the velocity vector (in tangential and the meridian plane) in a section behind the rotor blades.

3 Comparison of experimental and numerical results

As it was mentioned above, the axial distance between the stator blade trailing edge and the rotor blade leading edge corresponds with the configuration in which the flow field behind the stator blade was traversed with pneumatic probes in experimental research. It is therefore possible to compare results of the numerical simulation with the experimental data.

The experimental measurement was carried out on the test stand which is a part of the high-speed close-loop wind tunnel. This facility allows setting of the Reynolds and Mach number independently each other. A concept of the rotatable stator is used in consequence of linear probe manipulator. More details can be found in [2] and in [9-11].

Figures 12 to 15 show numerically calculated and measured flow fields in plane located in distance of 2 mm behind the trailing edge of the stator blade.

In figure 12 there are compared fields of the normalized kinetic energy losses, figure 13 shows comparison of the normalized Mach number fields and in figures 14 and 15 there are compared fields of two angles α and γ of the velocity vector.

One can see, that the numerical results fairly good correspond with the experimental data. There is a little difference in slope of the wake behind the stator blade as shown in figures 12 and 14. Figure 15 shows little more significant difference in distribution of the angle γ. To explain this fact will be paid attention in the follow-up work.

4 Conclusions

Calculations of flow in axial stage “REAC_v2-2” of the experimental reaction turbine were performed. The order of the axial turbine stage in multistage configuration was simulated through transferring of the radial distributions of the outlet flow field parameters on the inlet boundary

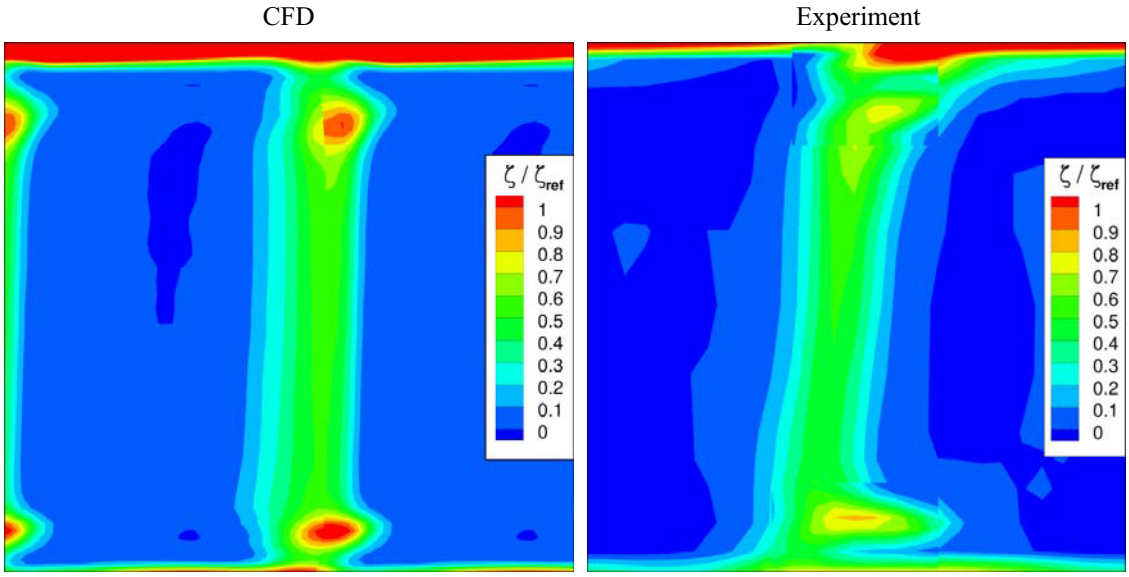

Fig. 12. Field of normalized kinetic energy losses in section behind the stator blades.

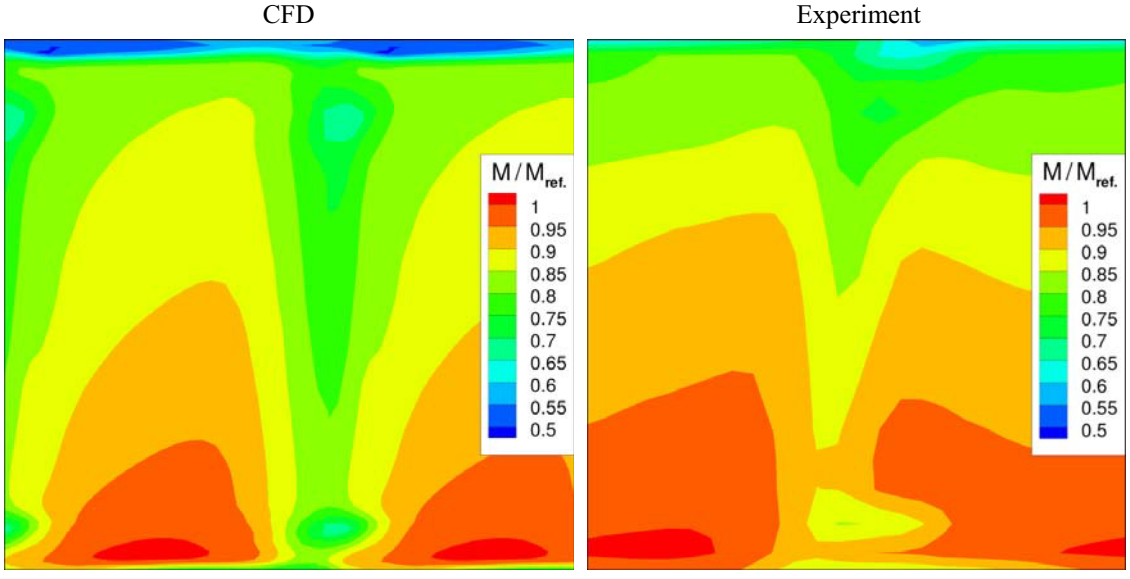

Fig. 13. Field of Mach number in section behind the stator blades.

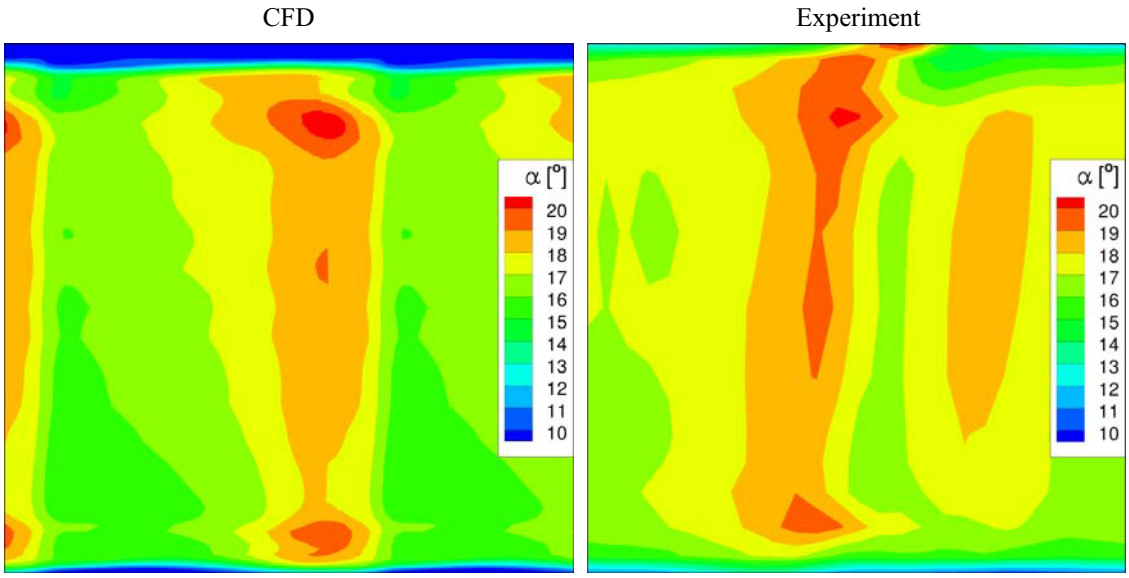

Fig. 14. Field of the angle α in tangential plane in section behind the stator blades.

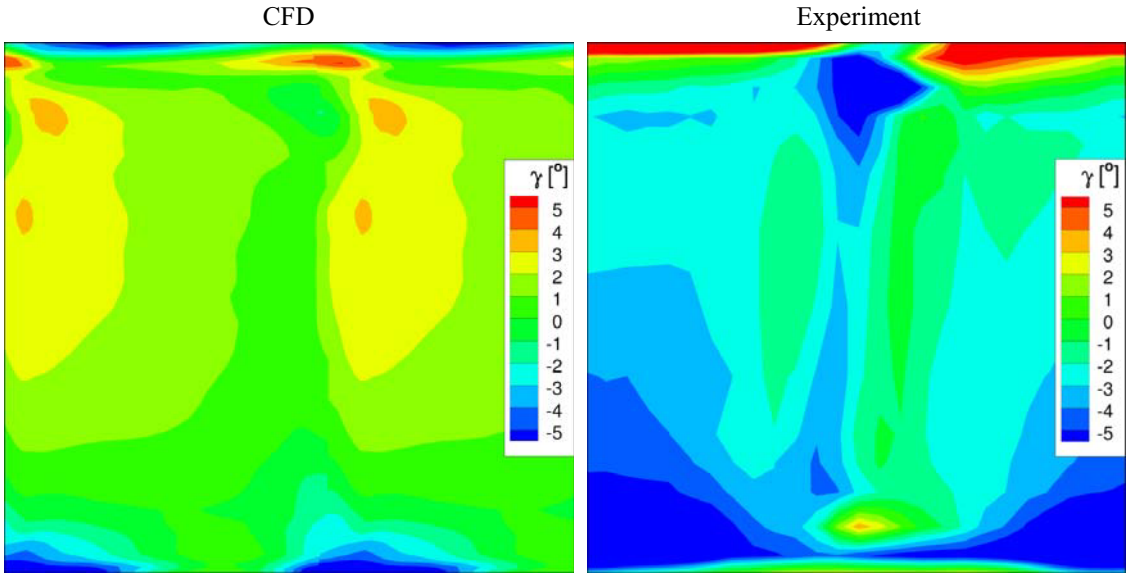

Fig. 15. Field of the angle γ in meridian plane in section behind the stator blades.

of the computational domain. It was found that the influence of the previous stage has the most effect on the flow field of the second stage. There were found some differences in the flow field of the third stage in area behind the stator blades, however, there are only minimal differences between outlet flow fields of the second and the third stage.

This work was supported by the Long-term Framework Advancement Plan provided by the Ministry of Industry and Trade of the Czech Republic and by the project TA04020129 of the Technology Agency of the Czech Republic.

References

1. https://www.rvvi.cz/cep?s=rozsirene-vyhledavani&ss=detail&n=0&h=TA04020129
2. http://www.vzlu.cz/cs/tunel-pro-turbomachinery-c74.html
3. T. Jelínek, P. Straka, V. Uruba, Proc. Conf. AENMFME 2016, pp. 77-80 (2016)
4. T. Jelínek, M. Němec, V. Uruba, Proc. Conf Engineering Mechanics 2016, pp. 254-257 (2016)
5. P. Straka, EPJ Web of conferences, **25**, 01090 (2012)
6. P. Straka, Report VZLÚ R-5904, Prague (2013), (in Czech)
7. P. Straka, Report VZLÚ R-4910, Prague (2010), (in Czech)
8. C.L. Rumsay, T.B. Gatski, Jour. Of Aircraft, **83**, pp. 904-910 (2001)
9. P. Straka, M. Němec, T. Jelínek, EPJ Web of conferences, **92**, 02088 (2015)
10. T. Jelínek, M. Němec, Turbomachinery 2010, Plzeň (2010) (in Czech)
11. M. Němec, T. Jelínek, J. Benetka, Report VZLÚ R-4939, Prague (2010) (in Czech)